Appendix A

A qualitative comparison of the first-order Born and Rytov approximations

A.1 Introduction

First-order Born and Rytov approximations are used to linearize the wave equation. The Born approximation produces a linear relation between the monochromatic, scattered wavefield $\Delta\Psi$ and a perturbed velocity field expressed as the object function O (where $\Psi = Ae^{i\phi}$, $\Delta\Psi = \Psi - \Psi_0$, and $O = {k_0}^2(1 - {v_0}^2/v^2)$). It transforms

$$\Delta\Psi(\mathbf{g}|\mathbf{s}) = \int O(\mathbf{r})G_0(\mathbf{g}-\mathbf{r})\{\Psi_0(\mathbf{r}|\mathbf{s}) + \Delta\Psi[\mathbf{r}|\mathbf{s}, O(\mathbf{r})]\}d\mathbf{r} \tag{A.1}$$

into

$$\Delta\Psi(\mathbf{g}|\mathbf{s}) = \int O(\mathbf{r})G_0(\mathbf{g}-\mathbf{r})\Psi_0(\mathbf{r}|\mathbf{s})d\mathbf{r}, \tag{A.2}$$

by assuming $\Delta\Psi << \Psi_0$. Since this weak-scattering approximation can be translated into into $|\Delta A/A_0| << 1$ and $|\Delta\phi| << 1$, the method requires both the total amount of scattering and the total change in phase to be small (Chernov, 1960).

The Rytov approximation produces a linear relation between the monochromatic scattered complex phase $\Delta\Phi$ and a perturbed velocity field (where $\Delta\Phi = \ln\Psi - \ln\Psi_0$). It

transforms

$$\Delta\Phi(\mathbf{g}|\mathbf{s}) = \int \frac{G_0(\mathbf{g}-\mathbf{r})\Psi_0(\mathbf{r}|\mathbf{s})}{\Psi_0(\mathbf{g}|\mathbf{s})}\{O(\mathbf{r}) + (\nabla(\Delta\Phi[\mathbf{r}|\mathbf{s}, O(\mathbf{r})]))^2\}d\mathbf{r}, \tag{A.3}$$

into

$$\Delta\Phi(\mathbf{g}|\mathbf{s}) = \int \frac{G_0(\mathbf{g}-\mathbf{r})\Psi_0(\mathbf{r}|\mathbf{s})}{\Psi_0(\mathbf{g}|\mathbf{s})}O(\mathbf{r})d\mathbf{r}, \tag{A.4}$$

by assuming $(\nabla(\Delta\Phi))^2 << O$. Since this smoothness assumption can be translated into $|\nabla \ln(A/A_0)/k_0| << 1$ and $|\nabla(\Delta\phi)/k_0| \leq 1$, the method requires both the amount of scattering per wavelength and the scattering angle to be small (Chernov, 1960).

In the weak-scattering limit the Born and Rytov approximations are equivalent; in the very-short-wavelength limit, the Rytov approximation reduces to the ray approximation (Devaney, 1981). Many papers have been written comparing the validity of the two approximations in the intermediate range. These papers fall into two groups. One group evaluates the approximations mathematically, comparing Born- and Rytov-modeled data with analytically modeled data (Keller, 1969; Oristaglio, 1987; Beydoun and Tarantola, 1987). The examples are limited to plane waves and plane interfaces. They demonstrate four main conclusions. First: since the Born approximation yields a linear relation between the scattered wavefield and the perturbed velocity model, it propagates energy with the background velocity model. Consequently, it is good at modeling energy reflected from a velocity perturbation that is small in magnitude, but it fails catastrophically at modeling energy transmitted through a velocity perturbation that is large in size (i.e., where the phase change through the object approaches a half wavelength). Second: because the Rytov approximation yields a linear relation between the scattered complex phase and the perturbed velocity model, it propagates energy with the perturbed velocity model. Consequently, it is good at modeling energy transmitted through a velocity perturbation that is small in magnitude, regardless of its size. Third: while the Rytov approximation models reflected energy with an error that is on the same order as that of the Born, it is inferior to the latter for this application. Rytov-modeled reflections equal Born-modeled reflections—plus additional weak, spurious events. Fourth: both approximations decrease in accuracy with increasing angle of incidence and/or velocity contrast.

The second group of papers evaluates the approximations by comparing the velocity inversions that result from their use in diffraction tomography (Slaney et al., 1984; Lo

et al., 1988). The examples are limited to localized anomalies in a constant background field. They demonstrate two conclusions. First: the Born approximation is better than the Rytov at determining the edges of a velocity anomaly (illuminated by reflected energy), and poorer at determining the interior of a velocity anomaly (illuminated by transmitted energy). Second: as the velocity perturbation increases and more and more energy is reflected, the Rytov approximation proves inferior to the Born.

This appendix falls into the second category, evaluating the Born and Rytov approximations by comparing their use in wave-equation tomography. The space-domain implementation and geometry of the examples are as described in chapter 4. A circular, two-dimensional anomaly is embedded in a homogeneous field, with a single source above and a line of receivers below. The velocity contrast of the slow anomaly is examined at 2.5%, 5.0% and 7.5%. In addition to a direct comparison of the resulting velocity inversions, the error terms in equations A.1 and A.3 are plotted for each example. While the conclusions are the same as those previously cited, examination of the error terms permits further insight into the differences between the Born and Rytov approximations.

A.2 Born Approximation

A.2.1 Velocity inversions

Figure A.1a shows the Born data measured for the experimental geometry of chapter 4. From top to bottom the rows correspond to frequencies of 5, 10, 15, 20 and 25 Hz. From left to right the columns correspond to slow velocity anomalies of magnitudes 2.5%, 5.0% and 7.5%. The solid and dashed lines show the imaginary and real parts of $\Delta\Psi$, as predicted by the Born approximation (equation A.2). The finely and coarsely dotted lines show the corresponding quantities measured in the finite-difference modeled data (equation A.1). Figure A.2a shows the Born-approximation velocity inversion produced by applying wave-equation tomography to the data of Figure A.1a. The rows and columns are the same as in the data figure, with two extensions. An additional column has been added on the left—the ideal inversion, generated by using data forward modeled with the Born approximation (the solid and dashed curves of Figure A.1a); an additional row has been added at the bottom—the inversions resulting from solving for all five frequencies simultaneously. The rows within each column are clipped at the maximum value of the ideal, multifrequency inversion for that anomaly magnitude: .0116, .0237, .0365. Because

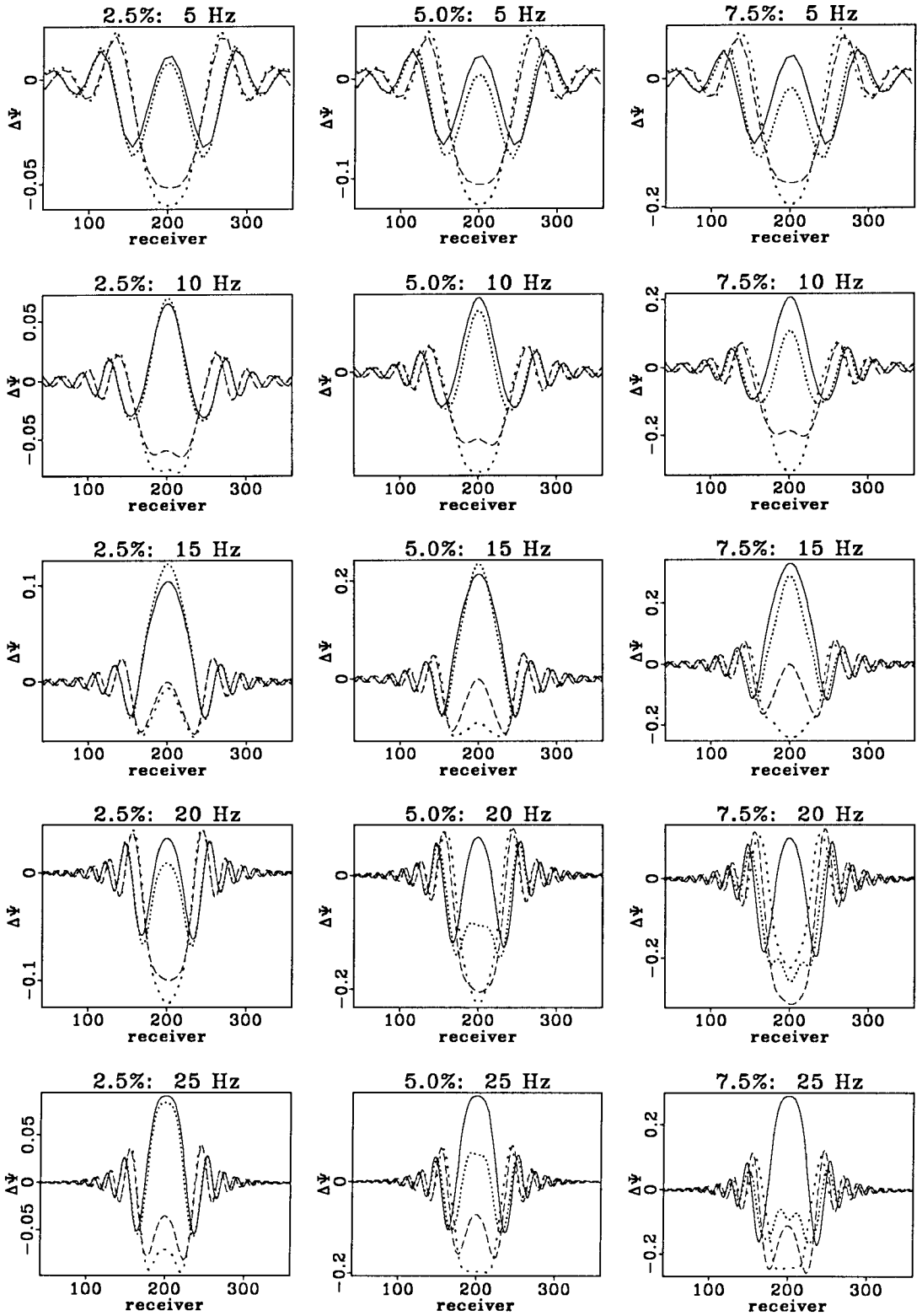

FIG. A.1. (a) Born data: the solid and dashed lines correspond to the imaginary and real parts of $\Delta\Psi$ predicted by the Born approximation; the finely and coarsely dotted lines correspond to the imaginary and real parts of $\Delta\Psi$ in the finite-difference generated data.

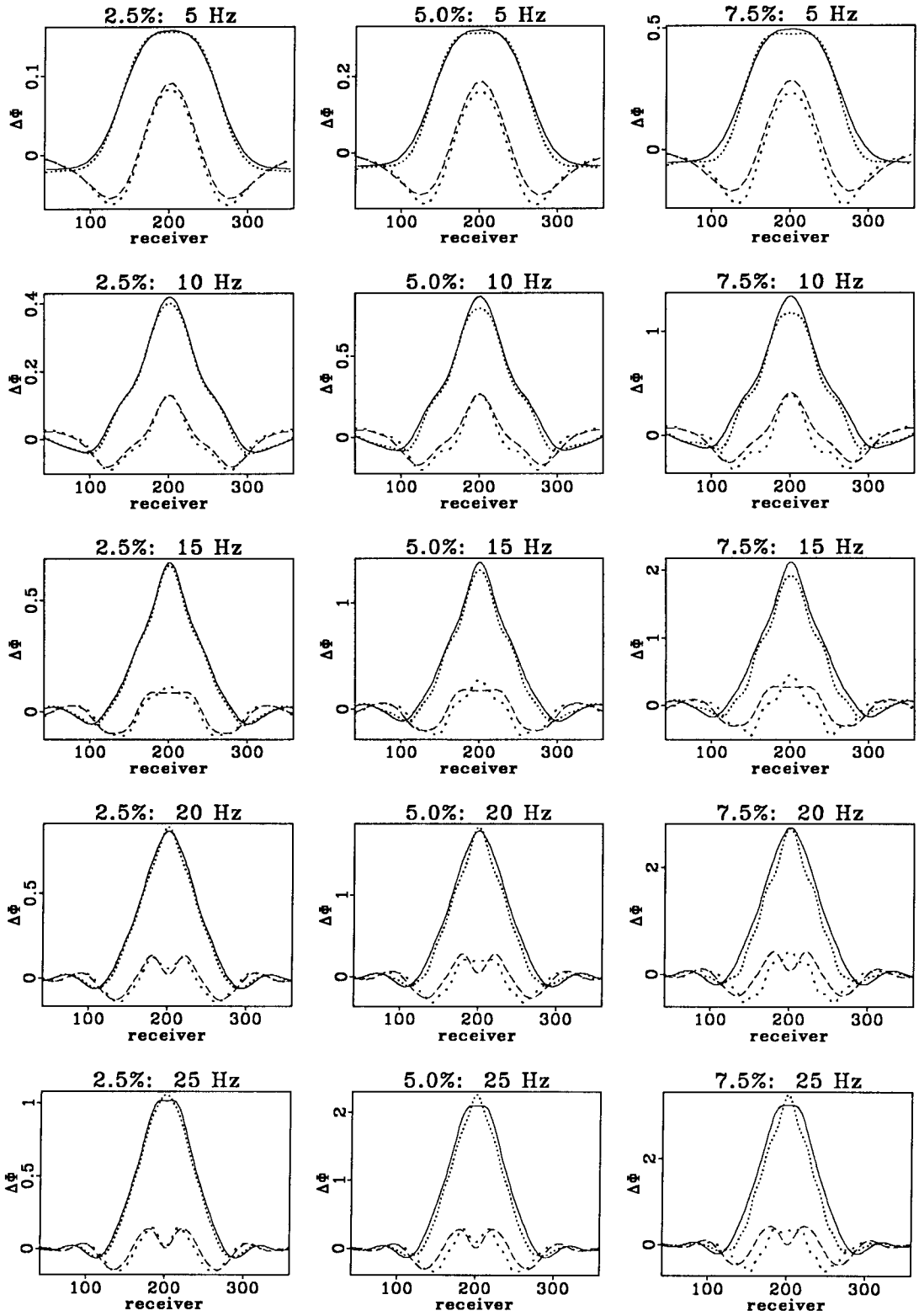

FIG. A.1. (b) Rytov data: the solid and dashed lines correspond to the imaginary and real parts of $\Delta\Phi$ predicted by the Rytov approximation; the finely and coarsely dotted lines correspond to the imaginary and real parts of $\Delta\Phi$ in the finite-difference generated data.

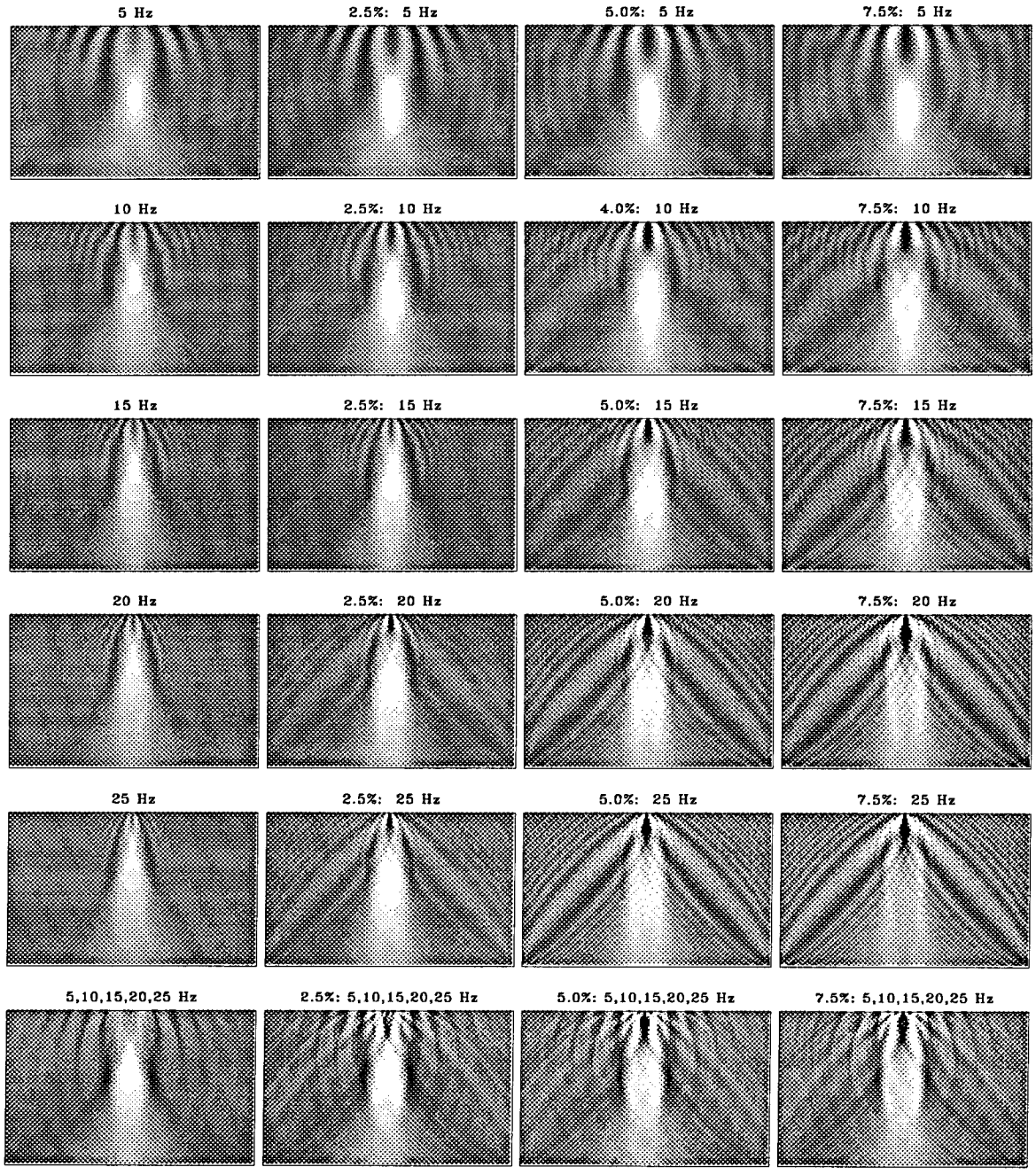

FIG. A.2. (a) Born-approximation velocity inversion.

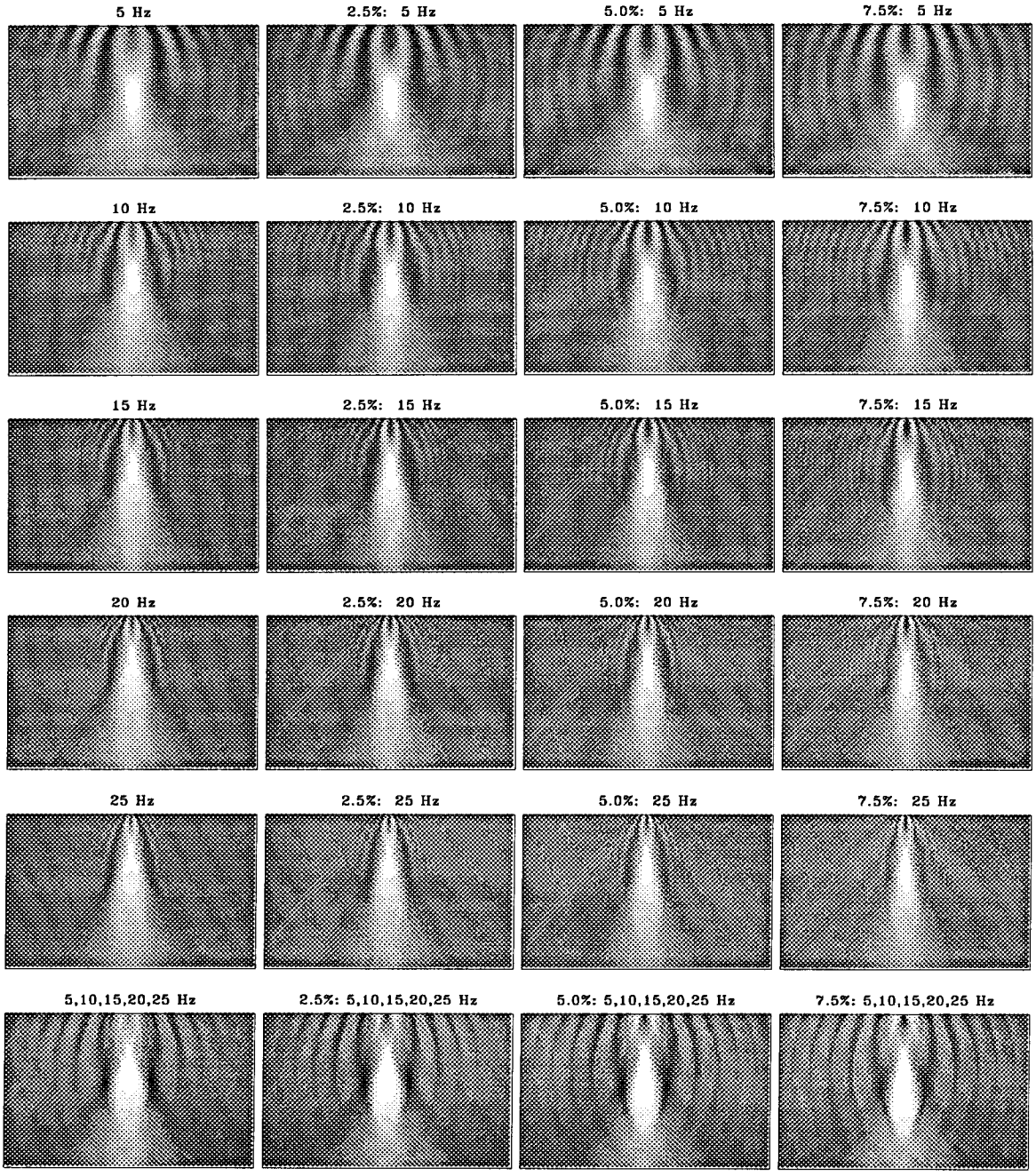

FIG. A.2. (b) Rytov-approximation velocity inversion.

the finite aperture of the experiment has smeared the energy over a broad region, these values are less than half the true anomaly magnitudes (.0256, .0526, .0811).

Two observations can be made about the figures. First, the error is larger for receivers directly below the source (transmitted energy) than for receivers to the side (reflected energy). In Figure A.2a this corresponds to the fact that the edges of the anomaly are determined even in the worst inversion (7.5% and 25 Hz), while the interior disappears. Second, the data error increases (and the inversions deteriorate) both with frequency and with anomaly magnitude. For a similar cylindrical anomaly, Slaney et al. (1984) observed that the Born approximation fails completely at describing transmission where the product of the relative refractive index ($\Delta v/v$) and the diameter of the cylinder exceeds .35λ. This limit is reached for the 7.5% anomaly at 20 Hz.

A.2.2 Error term

To facilitate comparison of Born and Rytov error terms, equation A.1 may be rewritten as:

$$\Delta\Psi(\mathbf{g}|\mathbf{s}) = \int G_0(\mathbf{g}-\mathbf{r})\Psi_0(\mathbf{r}|\mathbf{s})\left[O(\mathbf{r}) + \frac{O(\mathbf{r})\Delta\Psi[\mathbf{r}|\mathbf{s},O(\mathbf{r})]}{\Psi_0(\mathbf{r}|\mathbf{s})}\right] d\mathbf{r}. \tag{A.5}$$

Figure A.3a plots the complex absolute value of the error term of equation A.5, normalized by ${k_0}^2$:

$$\left|\frac{O\Delta\Psi}{{k_0}^2\Psi_0}\right|. \tag{A.6}$$

The rows and columns are as in Figure A.1a. Each panel is plotted full scale (without clipping). Figure A.4a shows the maximum value for each error panel: the horizontal axis is frequency; the solid, dashed and dotted lines correspond to 2.5%, 5.0% and 7.5% anomalies, respectively. Inspection of the error terms explains the results of Figures A.1a and A.2a. First, the error term's contribution to the integral in equation A.5 is confined within the boundaries of the anomaly. Consequently, the Born approximation is least accurate for the transmission experiment (when the source/receiver maxima of $G_0\Psi_0$—the interrogating wavepath—are closest to the anomaly), and most accurate for the reflection experiment (when the source/receiver maxima are far from the anomaly). Second, the error increases strongly with both frequency and velocity contrast. The error increases through the anomaly from top to bottom, as the phase difference between the background

and transmitted wavefields accumulates.

A.3 Rytov Approximation

A.3.1 Velocity inversions

Figures A.1b, A.2b and A.3b show the Rytov-approximation equivalents to Figures A.1a, A.2a and A.3a. In contrast to the Born approximation, the data and inversion errors in Figures A.1b and A.2b increase very slowly with anomaly magnitude (and reflectivity) and almost imperceptibly with frequency. Because the Rytov-predicted data are marginally more accurate for transmitted than reflected energy, the inverted images narrow marginally with frequency and anomaly magnitude: as the Rytov approximation finds the transmitting center and degrades the reflecting edges.

A.3.2 Error term

Figure A.3b is the Rytov approximation equivalent of Figure A.3a. It plots the complex absolute value of the error term of equation A.3, normalized by $k_0{}^2$:

$$\left| \frac{[\nabla(\Delta\Phi)]^2}{k_0{}^2} \right|. \tag{A.7}$$

In contrast to the Born-approximation results, the error term contributes to the integral in equation A.3 both inside and outside the anomaly. It is smallest inside the anomaly—as expected from the Rytov approximation's good transmission results. It is largest just beyond the edges of the anomaly—where the gradients of log relative-amplitude and phase delay are greatest. Figure A.4b is the Rytov equivalent of Figure A.4a. The maximum error increases with both frequency and velocity contrast, but much more slowly than with the Born approximation.

The morphology of the error term is reminiscent of the hyperbolas of Figure 3.10. A hyperbola describes the locus of points the difference of whose distances from two foci is constant. Since the anomaly acts as a secondary source (or focus), the striations in the error term coincide with curves of constant scattered phase, and therefore with curves of constant gradient in scattered phase. Note that for 5 and 10 Hz, where the anomaly is almost a point scatterer, the hyperbolas persist through the anomaly. Elsewhere, they are

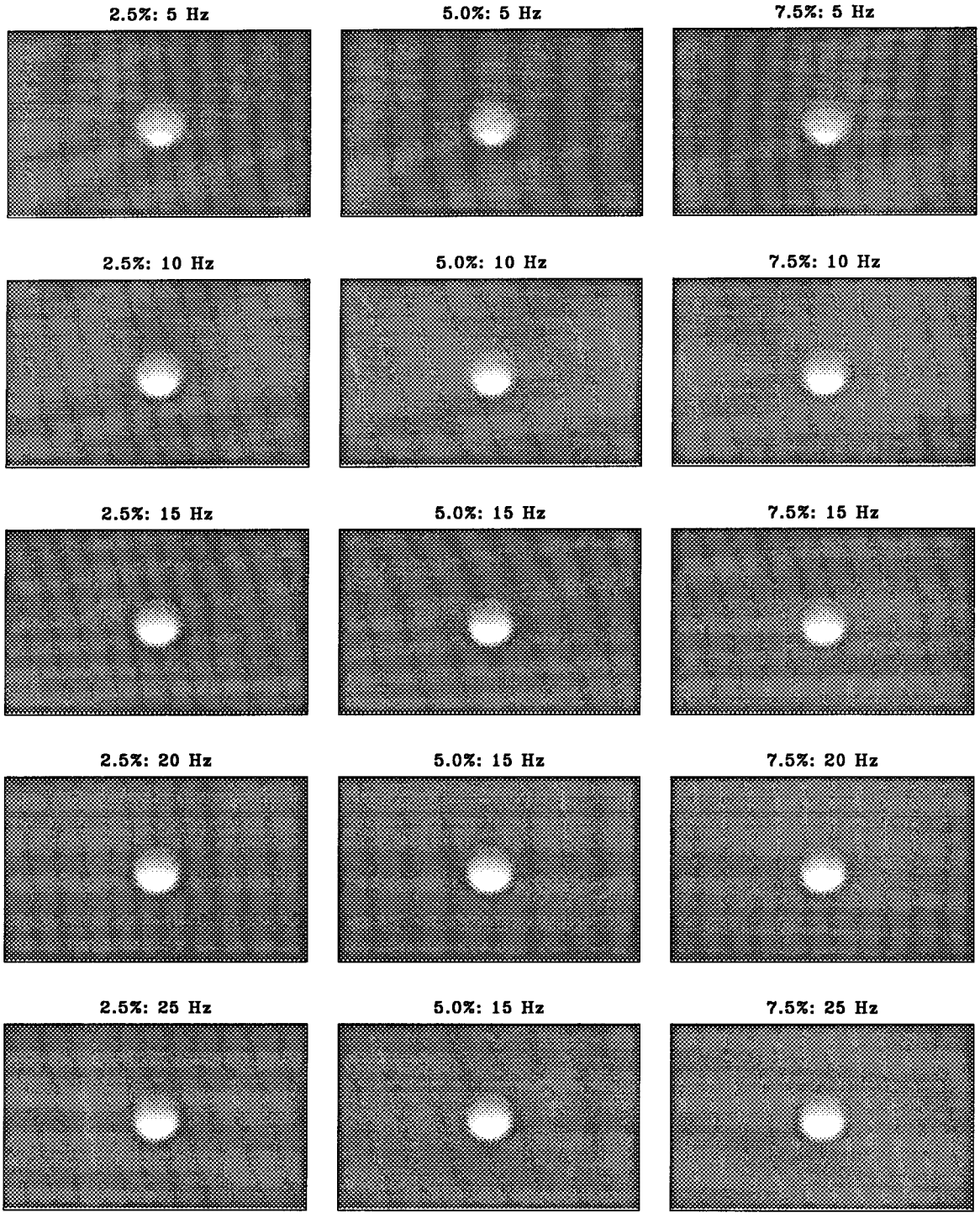

FIG. A.3. (a) Complex absolute value of the Born error term, normalized by $k_0{}^2$: $\left|\frac{O\Delta\Psi}{k_0{}^2\Psi_0}\right|$.

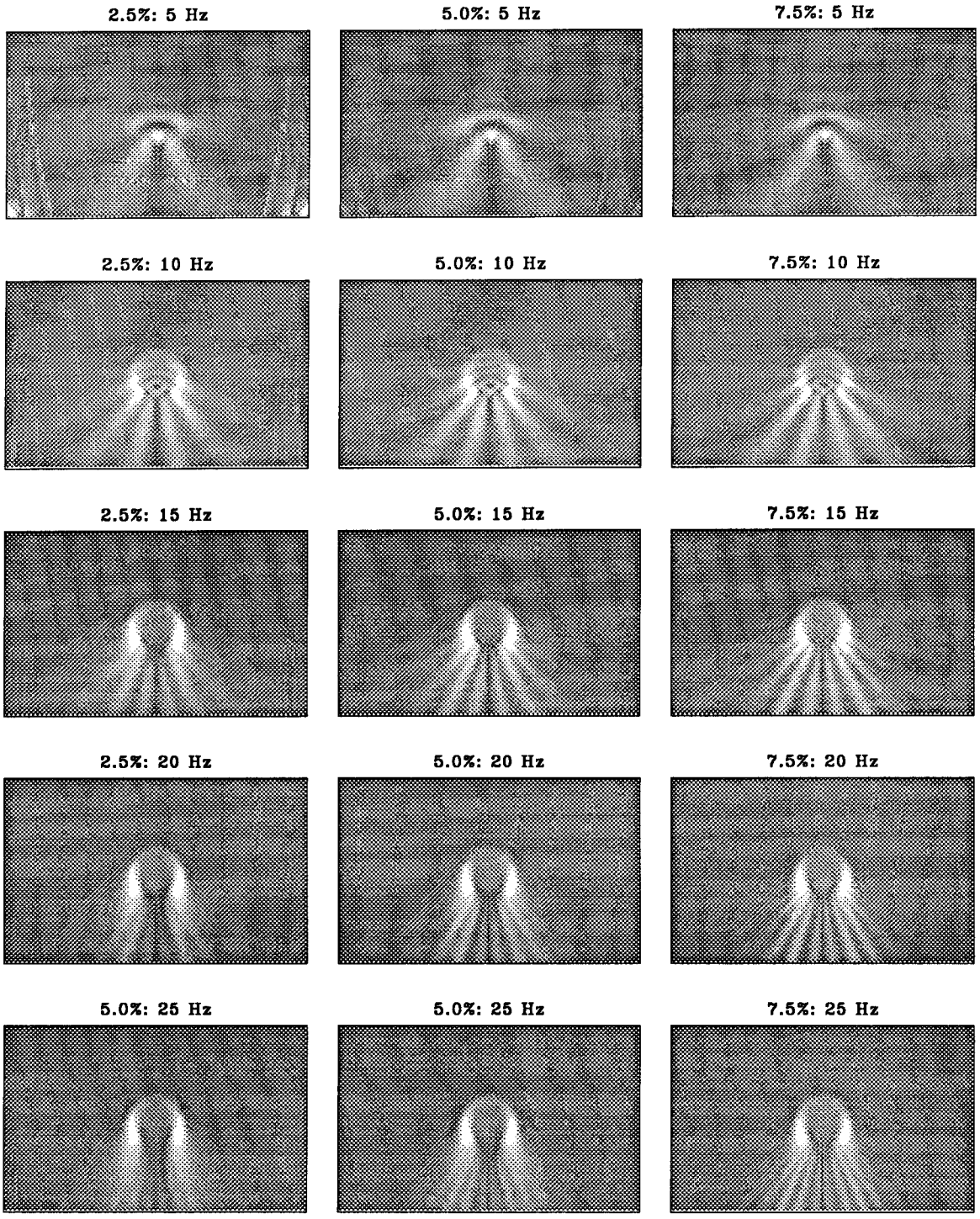

FIG. A.3. (b) Complex absolute value of the Rytov error term, normalized by $k_0{}^2$: $\left|\frac{(\nabla(\Delta\Phi))^2}{k_0{}^2}\right|$.

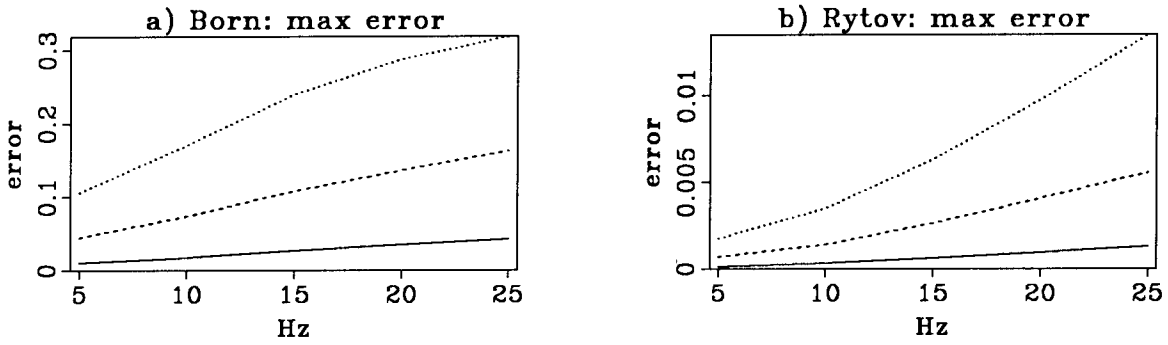

FIG. A.4. (a) Maximum value in Born error term: $\left|\frac{O\Delta\Psi}{k_0{}^2}\right|$; (b) Maximum value in Rytov error term: $\left|\frac{(\nabla(\Delta\Phi))^2}{k_0{}^2}\right|$. Solid, dashed and dotted lines correspond to anomaly magnitudes of 2.5%, 5.0%, and 7.5% respectively.

confined to its exterior. The arms increase in relative magnitude and extent with frequency and anomaly magnitude.

A.4 Conclusion

The superiority of the Rytov approximation for modeling transmitted energy assumes that perturbations to just one wave (e.g. the direct wave) are examined at one time. When perturbations to multiple waves (e.g. direct and reflected) are considered simultaneously, the linear relation between phase delay and transmission velocity breaks down—and the advantages of the Rytov over the Born approximation disappear (Keller, 1969). Consequently, successful application of the Rytov approximation requires isolation of both a single source wave and scattering from that wave. It should also be noted that application of the Rytov approximation is more difficult than application of the Born, because phase unwrapping must be performed.